The Role of Toll-like receptor 4 in respiratory syncytial virus replication, interferon lambda 1 induction, and chemokine responses.

Lindsay Broadbent[1], Jonathon D. Coey[1], Michael D. Shields[1,2], Ultan F. Power[1]

[1]Centre for Experimental Medicine, Queens University Belfast, 97 Lisburn Road, Belfast, Northern Ireland

[2] The Royal Belfast Hospital for Sick Children, Northern Ireland

Running title: RSV infection induces type III IFN through a TLR-4 dependent pathway

Corresponding address: Ultan F. Power, u.power@qub.ac.uk

Abstract

Respiratory syncytial virus (RSV) infection is the leading cause of severe lower respiratory tract infections (LRTI) in infants worldwide. The immune responses to RSV infection are implicated in RSV pathogenesis but RSV immunopathogenesis in humans remains poorly understood. We previously demonstrated that IFN-λ1 is the principle interferon induced following RSV infection of infants and well-differentiated primary pediatric bronchial epithelial cells (WD-PBECs). Interestingly, RSV F interacts with the TLR4/CD14/MD2 complex to initiate secretion of pro-inflammatory cytokines, while TLR4 stimulation with house dust mite induces IFN-λ1 production. However, the role of TLR4 in RSV infection and concomitant IFN-λ1 induction remains unclear. Using our RSV/WD-PBEC infection model, we found that CLI-095 inhibition of TLR4 resulted in significantly reduced viral growth kinetics, and secretion of IFN-λ1 and pro-inflammatory chemokines. To elucidate specific TLR4 signalling intermediates implicated in virus replication and innate immune responses we selected 4 inhibitors, including LY294002, U0126, SB203580 and JSH-23. SB203580, a p38 MAPK inhibitor, reduced both viral growth kinetics and IFN-λ1 secretion, while JSH-23, an NF-κB inhibitor, reduced IFN-λ1 secretion without affecting virus growth kinetics. Our data indicate that TLR4 plays a role in RSV entry and/or replication and IFN-λ1 induction following RSV infection is mediated, in part, by TLR4 signalling through NF-κB and/or p38 MAPK. Therefore, targeting TLR4 or downstream effector proteins could present novel treatment strategies against RSV.

Importance

The role of TLR4 in RSV infection and IFN-λ1 induction is controversial. Using our WD-PBEC model, which replicates many hallmarks of RSV infection *in vivo*, we demonstrated that the TLR4 pathway is involved in both RSV infection and/or

replication and the concomitant induction of IFN-λ1 and other pro-inflammatory cytokines. Increasing our understanding of the role of TLR4 in RSV immunopathogenesis may lead to the development of novel RSV therapeutics.

Introduction

Respiratory syncytial virus (RSV) is responsible for approximately 3.4 million hospitalisations of infants each year and is the primary cause of severe lower respiratory tract infections (LRTI) in children worldwide(1, 2). There are currently no RSV vaccines or specific therapeutics available. The innate immune system provides an important first line of defence against RSV disease. Innate immune signalling pathways are initiated by the recognition of pathogen associated molecular patterns (PAMPs) by cell surface or intracellular pathogen recognition receptors (PRRs), such as Toll-like receptors (TLRs). Some TLRs are implicated in activating innate immune responses following RSV infection. In particular, RSV F was shown to interact with the TLR4/CD14/MD2 complex, thereby initiating a signalling cascade leading to the induction of pro-inflammatory cytokines(3–5).

In infants hospitalised with RSV bronchiolitis TLR4 was shown to be upregulated on peripheral blood monocytes during the acute phase of the disease(6). However, the role of TLR4 in RSV infection and immunopathogenesis remains controversial. Some studies in mice demonstrated a TLR4-dependent innate immune response following RSV infection(3, 4, 7). Other studies in cell lines expressing human TLR4, however, reported that TLR4 did not play a significant role in RSV entry or NF-κB activation(8). The p38 MAPK pathway, which is downstream of TLR4, was implicated in RSV replication and was also shown to be involved in the expression of TLR4 near the site

of infection. Furthermore, inhibition of TLR4 resulted in a decrease in p38 MAPK activity(9).

We previously described well-differentiated primary pediatric bronchial epithelial cell (WD-PBEC) cultures that replicated many morphological and physiological hallmarks of bronchial epithelium *in vivo*, including ciliated epithelium and mucus producing goblet cells(10). Airway epithelium is the primary target for RSV infection *in vivo* (11). Importantly, we also demonstrated that RSV infection of WD-PBECs reproduces several hallmarks of RSV infection in infants. To date, much of the research to elucidate pathways leading to the induction of pro-inflammatory chemokines and cytokines following RSV infection has focused on the use of continuous cell lines or semi-permissive animal models. WD-PBECs evidently provide a more biologically relevant model in which to study innate immune responses to RSV infection of the human airway epithelium.

Our aim was to exploit our WD-PBEC model to investigate the role of TLR4 in RSV infection, the induction of type III IFNs, specifically IFN-λ1, and the production of pro-inflammatory chemokines by using specific inhibitors of TLR4 or downstream components of this pathway. CLI-095 is a potent and highly specific inhibitor of TLR4 signalling. It binds to Cys747 in the TLR4 intracellular domain but does not inhibit the binding of ligands to TLR4. CLI-095 binding disrupts the interaction of TLR4 with adaptor molecules, such as MyD88(12). We also exploited inhibitors of NF-κB (JSH-23), p38MAPK (SB203580), PI3K (LY294002), and MEK1/2 (U0126) to dissect signalling pathways implicated in RSV infection/replication and innate immune response induction.

We demonstrated that the intracellular signalling mediated by the TLR4 complex was involved in RSV infection/replication in WD-PBECs and initiated downstream innate immune responses, including type III IFNs and pro-inflammatory chemokines. p38 MAPK signalling was also implicated in RSV replication. Our data demonstrated that inhibition of TLR4 signalling decreases RSV-induced IFN-λ1 secretion. Furthermore, inhibition of p38 MAPK or NF-κB resulted in a reduction in RSV-induced IFN-λ1 secretion. As NF-κB inhibition did not affect RSV replication kinetics but diminished IFN-λ1 secretion, our data are consistent with an NF-κB-dependent mechanism of IFN-λ1 induction following RSV infection.

Results

To determine whether TLR4 influences RSV infection, HEK293 cells stably transfected with TLR4 or control HEK293/null cells were infected with RSV A2/eGFP (MOI~0.1). HEK293 cells do not endogenously express TLR4 (Figure 1A). The extent of eGFP fluorescence in the monolayers was used as a surrogate for the level of RSV infection. The kinetics and peak of eGFP spread throughout the monolayers was significantly higher in HEK293/TLR4 than in the HEK293/null cells, indicating that the presence of TLR4 increased the susceptibility of these cells to RSV infection (Figure 1B). We used CLI-095, a highly selective TLR4 signalling blocker, to investigate if it was the presence of TLR4 on the cell surface or the subsequent signalling cascade that was involved in the increase in RSV infection. CLI-095 does not affect ligand binding to TLR4 but inhibits all downstream signalling following TLR4 activation. CLI-095 (10 µg/mL) treatment of HEK293/TLR4 cells significantly reduced RSV growth kinetics compared to untreated HEK293/TLR4 controls, as

evidenced by eGFP fluorescence spread over time. At 48 hpi there was a significant difference between the level of eGFP expression in HEK293/null cells compared to HEK293/TLR4 ($p=0.006$) and HEK/TLR4 cells compared to HEK293/TLR4 vs HEK293/TLR4 + CLI-095 ($p=0.0152$). Similarly, at 72 hpi there was a significant difference between HEK293/null cells and HEK293/TLR4 ($p<0.0001$) and HEK/TLR4 compared to HEK293/TLR4 + CLI-095 ($p=0.0003$). In contrast, CLI-095 treatment of HEK293/null did not affect the spread of RSV infection, which was considerably lower than non-treated HEK293/TLR4 controls (Figure 1B).

To confirm whether these data were reproducible in a more physiologically relevant infection model, we exploited our RSV/WD-PBEC model (13, 14). WD-PBECs were stained to confirm the presence of TLR4 on the surface of these cells (Figure 2A). WD-PBECs were treated with varying concentrations of CLI-095 prior to infection with a low passage clinical isolate of RSV (RSV BT2a) (MOI=0.1). Consistent with the data from the HEK293/TLR4 cells, a dose-dependent reduction in RSV BT2a growth kinetics was observed (Figure 2B). The two highest concentrations of CLI-095 (10 and 100 µg/mL) resulted in significant reductions in viral titers over the course of the experiment. At the highest CLI-095 concentration used (100 µg/mL) mean RSV titres peaked at 3.09 $\log_{10}$ compared to 5.05 $\log_{10}$ in untreated controls. At 48, 72 and 96 hpi pre-treatment with 10 or 100 µg/mL CLI-095 resulted in a significant reduction in viral titres compared to the untreated infected controls.

Type III IFNs, in particular IFN-λ1, are the main interferons secreted following RSV infection (15). However, the mechanisms by which RSV induces type III IFN expression in epithelial cells is poorly understood. Evidence suggests that TLR4 may be implicated in the induction of type III IFNs following cell stimulation with house dust mite allergens (16). As the RSV F protein was shown to interact with the

TLR4/CD14/MD2 complex(8), we hypothesised that type III IFN induction following RSV infection was triggered following activation of the TLR4 pathway. To address this, the basolateral medium from CLI-095-pre-treated RSV BT2a-infected WD-PBECs was harvested from 72 to 120 hpi and the concentration of IFN-λ1 was determined. Treatment with both 10 and 100 μg/mL CLI-095 resulted in substantial reductions in IFN-λ1 secretions (Figure 2C) over the course of the experiment. There was a significant reduction in IFN-λ1 secretion following pre-treatment with 10 or 100 μg/mL CLI-095 at each time point, with the exception of 10 μg/mL at 72 hpi ($p=0.0549$). However, these CLI-095 concentrations also resulted in significant reductions in virus growth kinetics. If virus replication was essential for IFN-λ1 expression, inhibition of RSV infection/replication, rather than TLR4 signalling per se, might therefore explain the reduction in IFN-λ1 secretion.

To determine if the observed inhibition of RSV growth kinetics or IFN-λ1 production was dependent on specific TLR4 pathway intermediates, small molecule inhibitors directed against specific targets were used. WD-PBECs were treated with inhibitors for PI3K (LY294002), MEK1/2 (U0126), p38 MAPK (SB203580) or NF-κB (JSH-23), or DMSO as a control. Following infection with RSV BT2a, viral titers in apical rinses were quantified every 24 h until 96 hpi (Figure 3A). Inhibition of p38 MAPK resulted in a small but significant decrease in viral growth kinetics compared to the DMSO control. Conversely, MEK1/2 inhibition resulted in a significant increase in viral titers. Basal medium from these experiments was harvested and IFN-λ1 was quantified by ELISA. Significant decreases in IFN-λ1 concentrations were observed following inhibition of either p38MAPK or NF-κB (Figure 3B). In contrast, the significant increases in RSV growth kinetics evident following MEK1/2 inhibition did not result in concomitant increases in IFN-λ1 secretions. Interestingly, the only condition under which the IFN-

λ1 concentration was significantly impacted without altering viral titers was NF-κB inhibition, indicating that NF-κB plays an important role in RSV-induced IFN-λ1 induction.

RSV pathogenesis is mediated in large part by the pro-inflammatory immune responses to infection. Evidence suggests that the production of several chemokines, including IL-6 and CXCL8/IL-8, correlate with the severity of RSV disease in infants(17–20). To determine the consequences of TLR4 inhibition on RSV-induced chemokine secretion levels, WD-PBECs were pre-treated with CLI-095 followed by infection with RSV BT2a. Chemokine concentrations were determined in basal medium harvested at 48, 72 and 96 hpi. CLI-095 treatment prior to RSV infection resulted in significant reductions in MCP-1/CCL2, IL-8/CXCL8, IP-10/CXCL10 and IL-6 secretions in a dose-dependent manner relative to untreated controls (Figure 4).

Discussion

Previous publications reported that TLR4 signalling played no significant role in the entry and/or replication of RSV(8, 21). Surprisingly, our data indicated the contrary. We found a significant increase in the level of RSV infection in HEK293/TLR4 cells compared to HEK293/null cells. A number of experimental details may explain this discrepancy with the work of Marr and Turvey (2012)(8). First, while recombinant RSV A2 strains expressing eGFP were used in both studies, the *egfp* gene in our virus was inserted as the 1st transcription unit of the RSV genome, while it was inserted between the RSV *p* and *m* genes in rgRSV. This may have affected the respective virus replication kinetics in the cells. Second, we followed the spread of infection over a longer period of time. In the aforementioned manuscript, infection was followed only until 48 hpi, at which point a trend towards increased RSV spread was evident in

HEK293/TLR4 cells compared to HEK/null cells, but it did not reach significance. In contrast, we demonstrated significant differences at both 48 and 72 hpi in these same cell lines. Third, we exploited WD-PBECs and a low passage RSV clinical isolate, RSV BT2a, to confirm the role of TLR4 in RSV infection in a physiologically relevant model. Indeed, we also demonstrated a >2 $\log_{10}$ reduction in RSV titers following inhibition of TLR4 intracellular signalling in WD-PBECs with 100 µg/mL CLI-095. In contrast, much of the previous work exploited the use of cell lines that are permissive to RSV infection and can be easily transfected (8). Unlike our RSV/WD-PBEC model, these cell lines do not replicate the morphological or physiological complexities of differentiated airway epithelium, nor the cytopathogenesis of RSV in airway epithelium *in vivo*.

CLI-095 does not interfere with the external domain of TLR4. Therefore, we concluded that the internal portion of the TLR4 complex and/or the downstream signalling is associated with RSV growth kinetics in WD-PBECs. Our data from both immortalised cell lines and WD-PBECs indicated that TLR4 is implicated in RSV infection and/or replication. This is consistent with a recent report demonstrating a protective role of MEG3, a long noncoding RNA, against RSV infection, which most likely acts through the inhibition of the TLR4 signalling pathway(22).

Interestingly, TLR4 antagonists have been associated with a reduction in titers of other viruses both *in vitro* and *in vivo*. Indeed, eritoran, which binds to MD2 and prevents TLR4 activation, decreased viral titers, cytokine production, clinical symptoms and morbidity in a mouse model of influenza virus infection (23).

We demonstrated that CLI-095 possesses substantial prophylactic properties against RSV infection in our WD-PBEC model. As the inhibitor acts by blocking intracellular signalling and does not interfere with the extra-cellular domain of TLR4, it is unlikely

that CLI-095 interferes with the RSV F/TLR4 interaction. Indeed, Ii et al demonstrated that CLI-095 does not interfere with the binding of LPS to TLR4(24). As such, diminished RSV growth kinetics are unlikely to be due to the blocking of RSV F protein binding to the TLR4 complex. An association between TLR4 and nucleolin, a putative RSV co-receptor or entry factor, was recently described(25). Further work is needed to establish whether CLI-095 impacted the ability of RSV to interact with nucleolin and thereby, the ability of RSV to infect epithelial cells.

The TLR4 pathway, through adaptor proteins MyD88, TRAM and TRIF, was shown to activate innate immune responses following RSV infection, resulting in the downstream induction of pro-inflammatory cytokines/chemokines.(26) Although significant progress has recently been made in understanding the induction and function of type III IFNs, many questions remain unanswered. It is likely that there is cross-talk between the type I and type III IFN induction pathways, as well as compensatory mechanisms and a degree of redundancy between the two(27). As such, fully elucidating the type III IFN induction pathway has proven complicated. We demonstrated that pre-treatment of RSV-infected WD-PBECs with JSH-23, an NF-κB inhibitor, had a significant impact on the secretion of IFN-λ1 without affecting viral replication. Type III IFN can be induced through both NF-κB-dependent and independent pathways(28). Our data suggest that the induction of IFN-λ1 following RSV infection is, in part, due to NF-κB activation. However, JSH-23 treatment did not completely block IFN-λ1 secretion in response to RSV infection, thereby suggesting that there are other pathways through which RSV triggers IFN-λ1 induction. We also observed a reduction in IFN-λ1 secretion levels following pre-treatment with CLI-095 and SB203580, which were concomitant with significant reductions in viral growth kinetics. It is possible that diminished RSV replication could explain, in part, the

decrease in IFN-λ1 secretion. However, the absence of increased IFN-λ1 secretion following MEK1/2 inhibition, despite significantly increased RSV replication following U0126 treatment, suggest that RSV replication kinetics alone do not explain IFN-λ1 secretion levels. Further investigation is required to determine whether the reduction in IFN-λ1 secretion is due to diminished RSV replication or inhibition of TLR4 and/or p38 MAPK signalling, or both.

There is strong evidence to suggest that RSV pathogenesis is immune mediated(29–33). Higher concentrations of IL-6 and IL-8/CXCL8 in stimulated cord blood of infants is predictive of disease severity(19). Furthermore, DeVincenzo *et al*. correlated symptom scores with IL-6 and IL-8/CXCL8 secretion levels and with viral load in a human adult challenge model of RSV disease.(34). Our data demonstrated a reduction in both viral titers and proinflammatory chemokine production following CLI-095 pre-treatment. At the highest CLI-095 concentration used (100 μg/mL) there was a >2 $\log_{10}$ reduction in mean RSV titers compared to untreated controls. This reduction in viral replication coincided with a massive reduction in IP-10/CXCL10, MCP-1/CCL2 and IL-6 secretions and a significant reduction in IL-8/CXCL8. As these chemokines are implicated in RSV pathogenesis, our data are consistent with the concept that restricting RSV replication in infants to a level that poorly stimulates their secretion will alter the disease outcome, thereby providing the rationale for RSV prophylactics or early intervention therapeutics.

In conclusion, intra-cellular signalling mediated by the TLR4 complex was involved in the replication of RSV in WD-PBECs and initiated downstream innate immune responses, including type III IFNs and pro-inflammatory chemokines. Importantly, the TLR4 inhibitor, CLI-095 (or other similar molecules), may have potential as a RSV prophylactic, while our data provides the rationale for exploring its therapeutic potential

against RSV in WD-PBECs. p38 MAPK signalling is also implicated in RSV replication. Our data demonstrated that inhibition of TLR4 signalling decreases RSV-induced IFN-λ1 secretion. While the type III IFN induction pathway following RSV infection remains to be fully elucidated, our data demonstrated that both NF-κB and p38 MAPK are implicated. Increasing our understating of the innate immune responses to RSV will aid in the development of RSV prophylactics, therapeutics and vaccines.

Materials & Methods

Cell lines and viruses: The origin and characterization of the clinical isolate RSV BT2a were previously described (35). Recombinant RSV expressing eGFP (rRSV A2/eGFP) was a kind gift from Prof. Ralph Tripp (University of Georgia) and Prof. Michael Teng (University of South Florida). Its generation was previously described (36–38). The origin and characterization of the recent clinical isolate RSV BT2a were previously described(39). RSV titers in biological samples were determined as previously described(40). HEK293/TLR4 and HEK293/null cells were obtained from Invivogen and grown in DMEM (4.5 g/L glucose) supplemented with 10% HI-FBS. Cells were kept under selective pressure using blasticidin (Sigma Aldrich). HEK cells were infected for 2 h at 37^{o}C in DMEM (4.5 g/L glucose, 0% FBS) then maintained in serum-free DMEM (4.5 g/L glucose).

WD-PBEC cultures: Passage 1 primary paediatric bronchial epithelial cells (PBECs) were obtained commercially (Lonza). WD-PBEC cultures were generated as described previously(14) . Complete differentiation took a minimum of 21 days. Cultures were only used when hallmarks of excellent differentiation were evident, including, no holes in the cultures, extensive apical coverage with beating cilia, and

obvious mucus production. WD-PBECs were infected apically for 2 h at 37ºC. For apical rinses of WD-PBECs during experimentation low glucose DMEM was added apically (200 µL) and left for 5 min at room temperature (RT). This was aspirated without damaging the cultures, added to cryovials and snap frozen in liquid nitrogen. At specified intervals post-treatment and/or infection basolateral medium was also harvested and snap frozen in liquid nitrogen, and replaced with fresh medium.

Immunofluorescence: HEK293/null, HEK293/TLR4 cells and WD-PBECs were fixed with 4% PFA (v/v in PBS) for 40 mins then permeabilised with 0.1% Triton X-100 (v/v in PBS) for 1 h. Cells were blocked with 0.4% BSA (v/v in PBS) for 30 mins then incubated with anti-TLR4 antibody (Santa Cruz) overnight at 4ºC. Following washing, cells were incubated with goat anti-rabbit AlexaFluor 488 antibody for 1 h at 37ºC. Cultures were mounted with DAPI mounting medium (Vectashield, Vector Labs) and imaged using a Nikon Eclipse 90i.

Signalling inhibitors: All of the inhibitors were reconstituted in DMSO (Sigma Aldrich) as per the manufacturers' instructions. Concentrations of all inhibitors used for these experiments were at least double the IC_{50} (inhibitory concentration 50%) indicated by the manufacturer. Stocks were diluted in ALI medium to achieve the working concentration. WD-PBECs were pre-treated apically at 37ºC for the time indicated in figure legends.

The inhibitors used were:

(i) CLI-095 (Source Bioscience), a TLR4 inhibitor that blocks the intracellular signalling, but not the extracellular domain. Concentrations used are stated in individual figure legends.

(ii) LY294002 (50 µM) (LC labs), a PI3K reversible inhibitor that inhibits Akt/PKB signalling. It also inhibits cell proliferation and induces apoptosis.

(iii) U0126 (20 µM) (LC labs), a highly selective inhibitor of MEK1/2. Acts by disrupting the transcriptional activity of AP-1 and blocks the downstream induction of cytokines and MMPs.

(iv) SB203580 (1 µM) (Sigma Aldrich), a p38 MAPK inhibitor that also blocks PBK phosphorylation and total SAPK/JNK activity. At high concentrations it has been shown to activate the ERK pathway and lead to an increase in NF-κB activity.

(v) JSH-23 (20 µM) (Sigma Aldrich), is an NF-κB inhibitor. It has also been shown, under certain conditions, to inhibit apoptotic chromatin condensation and NO production.

IFN-λ1 quantification: IFN-λ1 ELISA kits were purchased from eBioscience (Ready to use Platinum Sandwich ELISA kit). IFN-λ1 was quantified from basolateral medium harvested from WD-PBECs, following the manufacturer's instructions. Frozen aliquots of basolateral medium were rapidly defrosted in a water bath at 37^{o}C and kept on ice during the ELISA procedure to minimise degradation.

Chemokine quantification: ProcartaPlex kits were purchased from eBioscience to measure a panel of chemokines present in basolateral medium. The manufacturer's protocol was followed throughout. Analytes measured included IP-10/CXCL10, IL-8/CXCL8, IL-6, and MCP-1/CCL2.

Image analysis: Image analysis was carried out using ImageJ software (http://rsbweb.nih.gov/ij/). A minimum of 5 fields were captured per condition/well by UV microscopy (Nikon TE-2000U and Hammamatsu Orca-ER camera).

Statistical analysis: GraphPad Prism ® was used to create graphical representations of the data and for statistical analyses. Summary measures over

time were compared by calculating the areas under the curves (AUC) and we used t tests to calculate if these AUCs were statistically significantly different. Differences were also assessed by unadjusted t tests at each time point.

$p<0.05$ was considered significant.

* p value = <0.05; ** p value = <0.01; *** p value = <0.001.

References

1. Nair H, Brooks WA, Katz M, Roca A, Berkley JA, Madhi SA, Simmerman JM, Gordon A, Sato M, Howie S, Krishnan A, Ope M, Lindblade KA, Carosone-Link P, Lucero M, Ochieng W, Kamimoto L, Dueger E, Bhat N, Vong S, Theodoratou E, Chittaganpitch M, Chimah O, Balmaseda A, Buchy P, Harris E, Evans V, Katayose M, Gaur B, O'Callaghan-Gordo C, Goswami D, Arvelo W, Venter M, Briese T, Tokarz R, Widdowson M-A, Mounts AW, Breiman RF, Feikin DR, Klugman KP, Olsen SJ, Gessner BD, Wright PF, Rudan I, Broor S, Simões EAF, Campbell H. 2011. Global burden of respiratory infections due to seasonal influenza in young children: a systematic review and meta-analysis. Lancet 378:1917–30.

2. Lotz MT, Peebles RS. 2012. Mechanisms of respiratory syncytial virus modulation of airway immune responses. Curr Allergy Asthma Rep 12:380–7.

3. Haynes LM, Moore DD, Kurt-Jones EA, Finberg RW, Anderson LJ, Tripp RA. 2001. Involvement of toll-like receptor 4 in innate immunity to respiratory syncytial virus. J Virol 75:10730–7.

4. Kurt-Jones EA, Popova L, Kwinn L, Haynes LM, Jones LP, Tripp RA, Walsh

EE, Freeman MW, Golenbock DT, Anderson LJ, Finberg RW. 2000. Pattern recognition receptors TLR4 and CD14 mediate response to respiratory syncytial virus. Nat Immunol 1:398–401.

5. Rallabhandi P, Bell J, Boukhvalova MS, Medvedev A, Lorenz E, Arditi M, Hemming VG, Blanco JCG, Segal DM, Vogel SN. 2006. Analysis of TLR4 polymorphic variants: new insights into TLR4/MD-2/CD14 stoichiometry, structure, and signaling. J Immunol 177:322–32.

6. Gagro A, Tominac M, Krsulović-Hresić V, Baće A, Matić M, Drazenović V, Mlinarić-Galinović G, Kosor E, Gotovac K, Bolanca I, Batinica S, Rabatić S. 2004. Increased Toll-like receptor 4 expression in infants with respiratory syncytial virus bronchiolitis. Clin Exp Immunol 135:267–72.

7. Haeberle HA, Takizawa R, Casola A, Brasier AR, Dieterich H-J, Van Rooijen N, Gatalica Z, Garofalo RP. 2002. Respiratory syncytial virus-induced activation of nuclear factor-kappaB in the lung involves alveolar macrophages and toll-like receptor 4-dependent pathways. J Infect Dis 186:1199–206.

8. Marr N, Turvey SE. 2012. Role of human TLR4 in respiratory syncytial virus-induced NF- B activation, viral entry and replication. Innate Immun 18:856–865.

9. Marchant D, Singhera GK, Utokaparch S, Hackett TL, Boyd JH, Luo Z, Si X, Dorscheid DR, McManus BM, Hegele RG. 2010. Toll-Like Receptor 4-Mediated Activation of p38 Mitogen-Activated Protein Kinase Is a Determinant of Respiratory Virus Entry and Tropism. J Virol 84:11359–11373.

10. Villenave R, Thavagnanam S, Sarlang S, Parker J, Douglas I, Skibinski G, Heaney LG, McKaigue JP, Coyle P V, Shields MD, Power UF. 2012. In vitro

384 modeling of respiratory syncytial virus infection of pediatric bronchial
385 epithelium, the primary target of infection in vivo. Proc Natl Acad Sci U S A
386 109:5040–5.

387 11. Zhang L, Peeples ME, Boucher RC, Collins PL, Pickles RJ. 2002. Respiratory
388 syncytial virus infection of human airway epithelial cells is polarized, specific to
389 ciliated cells, and without obvious cytopathology. J Virol 76:5654–66.

390 12. Matsunaga N, Tsuchimori N, Matsumoto T, Ii M. 2011. TAK-242 (resatorvid), a
391 small-molecule inhibitor of Toll-like receptor (TLR) 4 signaling, binds
392 selectively to TLR4 and interferes with interactions between TLR4 and its
393 adaptor molecules. Mol Pharmacol 79:34–41.

394 13. Villenave R, Touzelet O, Thavagnanam S, Sarlang S, Parker J, Skibinski G,
395 Heaney LG, McKaigue JP, Coyle P V, Shields MD, Power UF. 2010.
396 Cytopathogenesis of Sendai virus in well-differentiated primary pediatric
397 bronchial epithelial cells. J Virol 84:11718–28.

398 14. Broadbent L, Villenave R, Guo-Parke H, Douglas I, Shields MD, Power UF.
399 2016. In Vitro Modeling of RSV Infection and Cytopathogenesis in Well-
400 Differentiated Human Primary Airway Epithelial Cells (WD-PAECs)., p. 119–
401 39. *In* Methods in molecular biology (Clifton, N.J.).

402 15. Villenave R, Broadbent L, Douglas I, Lyons JD, Coyle P V., Teng MN, Tripp
403 RA, Heaney LG, Shields MD, Power UF. 2015. Induction and Antagonism of
404 Antiviral Responses in Respiratory Syncytial Virus-Infected Pediatric Airway
405 Epithelium. J Virol 89:12309–12318.

406 16. Hammad H, Chieppa M, Perros F, Willart MA, Germain RN, Lambrecht BN.
407 2009. House dust mite allergen induces asthma via Toll-like receptor 4

triggering of airway structural cells. Nat Med 15:410–6.

17. McNamara PS, Flanagan BF, Hart CA, Smyth RL. 2005. Production of chemokines in the lungs of infants with severe respiratory syncytial virus bronchiolitis. J Infect Dis 191:1225–32.

18. Murai H, Terada A, Mizuno M, Asai M, Hirabayashi Y, Shimizu S, Morishita T, Kakita H, Hussein MH, Ito T, Kato I, Asai K, Togari H. 2007. IL-10 and RANTES are elevated in nasopharyngeal secretions of children with respiratory syncytial virus infection. Allergol Int 56:157–63.

19. Juntti H, Osterlund P, Kokkonen J, Dunder T, Renko M, Pokka T, Julkunen I, Uhari M. 2009. Cytokine responses in cord blood predict the severity of later respiratory syncytial virus infection. J Allergy Clin Immunol 124:52-58.e1–2.

20. Tabarani CM, Bonville C a, Suryadevara M, Branigan P, Wang D, Huang D, Rosenberg HF, Domachowske JB. 2013. Novel inflammatory markers, clinical risk factors and virus type associated with severe respiratory syncytial virus infection. Pediatr Infect Dis J 32:e437-42.

21. Lizundia R, Sauter K-S, Taylor G, Werling D. 2008. Host species-specific usage of the TLR4-LPS receptor complex. Innate Immun 14:223–31.

22. Tao X, Zeng L, Wang H, Liu H. 2017. LncRNA MEG3 ameliorates respiratory syncytial virus infection by suppressing TLR4 signaling. Mol Med Rep 17:4138–4144.

23. Shirey KA, Lai W, Scott AJ, Lipsky M, Mistry P, Pletneva LM, Karp CL, McAlees J, Gioannini TL, Weiss J, Chen WH, Ernst RK, Rossignol DP, Gusovsky F, Blanco JCG, Vogel SN. 2013. The TLR4 antagonist Eritoran protects mice from lethal influenza infection. Nature 497:498–502.

24. Ii M, Matsunaga N, Hazeki K, Nakamura K, Takashima K, Seya T, Hazeki O, Kitazaki T, Iizawa Y. 2006. A novel cyclohexene derivative, ethyl (6R)-6-[N-(2-Chloro-4-fluorophenyl)sulfamoyl]cyclohex-1-ene-1-carboxylate (TAK-242), selectively inhibits toll-like receptor 4-mediated cytokine production through suppression of intracellular signaling. Mol Pharmacol 69:1288–95.

25. Yuan X, Hu T, He H, Qiu H, Wu X, Chen J, Wang M, Chen C, Huang S. 2018. Respiratory syncytial virus prolifically infects N2a neuronal cells, leading to TLR4 and nucleolin protein modulations and RSV F protein co-localization with TLR4 and nucleolin. J Biomed Sci 25:13.

26. Zhou Y, Yang J, Deng H, Xu H, Zhang J, Jin W, Gao H, Liu F, Zhao D. 2014. Respiratory syncytial virus infection modulates interleukin-8 production in respiratory epithelial cells through a transcription factor-activator protein-1 signaling pathway. Mol Med Rep 10:1443–7.

27. Ioannidis I, Ye F, McNally B, Willette M, Flaño E. 2013. Toll-like receptor expression and induction of type I and type III interferons in primary airway epithelial cells. J Virol 87:3261–70.

28. Thomson SJP, Goh FG, Banks H, Krausgruber T, Kotenko S V, Foxwell BMJ, Udalova IA. 2009. The role of transposable elements in the regulation of IFN-lambda1 gene expression. Proc Natl Acad Sci U S A 106:11564–9.

29. Selvaggi C, Pierangeli A, Fabiani M, Spano L, Nicolai A, Papoff P, Moretti C, Midulla F, Antonelli G, Scagnolari C. 2014. Interferon lambda 1-3 expression in infants hospitalized for RSV or HRV associated bronchiolitis. J Infect 68:467–77.

30. Moreno-Solís G, Torres-Borrego J, de la Torre-Aguilar MJ, Fernández-

Gutiérrez F, Llorente-Cantarero FJ, Pérez-Navero JL. 2014. Analysis of the local and systemic inflammatory response in hospitalized infants with respiratory syncitial virus bronchiolitis. Allergol Immunopathol (Madr).

31. Díaz P V, Gaggero AA, Pinto RA, Mamani R, Uasapud PA, Bono MR. 2013. Aumento de interleuquinas proinflamatorias y de cortisol plasmático en bronquiolitis por virus respiratorio sincicial: relación con la gravedad de la infección. Rev Med Chil 141:574–581.

32. Tapia LI, Ampuero S, Palomino MA, Luchsinger V, Aguilar N, Ayarza E, Mamani R, Larrañaga C. 2013. Respiratory syncytial virus infection and recurrent wheezing in Chilean infants: a genetic background? Infect Genet Evol 16:54–61.

33. García C, Soriano-Fallas A, Lozano J, Leos N, Gomez AM, Ramilo O, Mejias A. 2012. Decreased innate immune cytokine responses correlate with disease severity in children with respiratory syncytial virus and human rhinovirus bronchiolitis. Pediatr Infect Dis J 31:86–9.

34. DeVincenzo JP, Wilkinson T, Vaishnaw A, Cehelsky J, Meyers R, Nochur S, Harrison L, Meeking P, Mann A, Moane E, Oxford J, Pareek R, Moore R, Walsh E, Studholme R, Dorsett P, Alvarez R, Lambkin-Williams R. 2010. Viral load drives disease in humans experimentally infected with respiratory syncytial virus. Am J Respir Crit Care Med 182:1305–14.

35. Villenave R, O'Donoghue D, Thavagnanam S, Touzelet O, Skibinski G, Heaney LG, McKaigue JP, Coyle P V, Shields MD, Power UF. 2011. Differential cytopathogenesis of respiratory syncytial virus prototypic and clinical isolates in primary pediatric bronchial epithelial cells. Virol J 8:43.

480 36. Techaarpornkul S, Barretto N, Peeples ME. 2001. Functional analysis of
481 recombinant respiratory syncytial virus deletion mutants lacking the small
482 hydrophobic and/or attachment glycoprotein gene. J Virol 75:6825–34.

483 37. Collins PL, Hill MG, Camargo E, Grosfeld H, Chanock RM, Murphy BR. 1995.
484 Production of infectious human respiratory syncytial virus from cloned cDNA
485 confirms an essential role for the transcription elongation factor from the 5'
486 proximal open reading frame of the M2 mRNA in gene expression and
487 provides a capability for vaccine . Proc Natl Acad Sci U S A 92:11563–7.

488 38. Ling Z, Tran KC, Teng MN. 2009. Human respiratory syncytial virus
489 nonstructural protein NS2 antagonizes the activation of beta interferon
490 transcription by interacting with RIG-I. J Virol 83:3734–42.

491 39. Villenave R, O'Donoghue D, Thavagnanam S, Touzelet O, Skibinski G,
492 Heaney LG, McKaigue JP, Coyle P V, Shields MD, Power UF. 2011.
493 Differential cytopathogenesis of respiratory syncytial virus prototypic and
494 clinical isolates in primary pediatric bronchial epithelial cells. Virol J 8:43.

495 40. Power UF, Plotnicky-Gilquin H, Huss T, Robert A, Trudel M, Stahl S, Uhlen M,
496 Nguyen TN, Binz H. 1997. Induction of protective immunity in rodents by
497 vaccination with a prokaryotically expressed recombinant fusion protein
498 containing a respiratory syncytial virus G protein fragment. Virology 230:155–
499 166.

500

501

Figure Legends

Figure 1. To confirm the presence/absence of TLR4 HEK293 cells stably transfected with TLR4 or null control cells were fixed using 4% PFA (v/v in PBS) then permeabilised using 0.1% Triton X-100 (v/v in PBS) for 1 h. Cells were incubated with anti-TLR4 antibody (Santa Cruz) followed by a green secondary antibody (AlexaFluor) (A). HEK293/null and HEK293/TLR4 cells were treated with 10 µg/mL CLI-095 or mock treated for 6 h then infected (in duplicate) with RSV/eGFP at an MOI=0.1. Five images per well were captured at 24, 48 and 72 hpi using a Nikon TE2000U microscope. The % of the image expressing green fluorescence was assessed using Image J. The average of the 5 fields of view per well was calculated (B). The data were derived from 2 independent experiments carried out in duplicate. Vertical dotted lines indicate statistical significance when areas under the curves were calculated and compared (** p value = <0.01; *** p value = <0.001). Differences were also assessed by t test at each time point.

Figure 2. To confirm the presence of TLR4 on WD-PBECs uninfected cultures were fixed using 4% PFA (v/v in PBS) permeabilised then using 0.1% Triton X-100 (v/v in PBS) for 1 h. Cells were incubated with anti-TLR4 antibody (Santa Cruz) followed by a green secondary antibody (AlexaFluor) (A). WD-PBECs (n=3 donors, duplicate Transwells for each condition), pre-treated apically with 1, 10 or 100 µg/mL CLI-095 or untreated, were infected with RSV BT2a (MOI=0.1). Apical washes were harvested every 24 h following infection up to 96 hpi; 200 µL DMEM (with no additives) was incubated on the apical surface for 5 min at RT, removed and snap frozen in liquid nitrogen. Basal medium was also harvested every 24 h. Apical washes were titrated on HEp-2 cells to determine virus growth kinetics (B). IFN-λ1 in basolateral medium from wells, pre-treated with 10 or 100 µg/mL CLI-095 or untreated at 72, 96 and 120 hpi, was quantified by ELISA (eBioscience) (C). Vertical dotted lines indicate statistical

significance when areas under the curves were calculated and compared (** p value = <0.01; *** p value = <0.001). Statistical significance between conditions was also assessed at each time point.

Figure 3. WD-PBECs (n=3 donors) were pre-treated apically with LY294002 (PI3K inhibitor), U0126 (MEK1/2 inhibitor), SB203580 (p38MAPK inhibotor), JSH-23 (NF-κB inhibitor), or DMSO (used as a control) for 1 h at 37°C prior to infection with RSV BT2a (MOI=0.1). Apical washes were harvested every 24 h following infection and titrated on HEp-2 cells to determine virus growth kinetics (A). Basolateral medium was harvested and replaced with fresh medium every 24 h. IFN-λ1 in basolateral medium harvested at 48, 72, 96 and 120 hpi was quantified by ELISA (eBioscience) (B). Vertical dotted lines indicate statistical significance when areas under the curves were calculated and compared * p value = <0.05; ** p value = <0.01).

Figure 4. WD-PBECs (n=3 donors), pre-treated apically with 10 or 100 μg/mL CLI-095 or untreated, were infected with RSV BT2a at an MOI=0.1. Basolateral medium was harvested and replaced with fresh medium every 24 h. The concentration of MCP-1/CCL2, IP-10/CXCL10, IL-6 and IL-8/CXCL8 in basolateral medium was measured by BioPlex (eBioscience) at 48, 72 and 96 hpi. Vertical dotted lines indicate statistical significance when areas under the curves were calculated and compared * p value = <0.05; ** p value = <0.01).

FIG 1

A

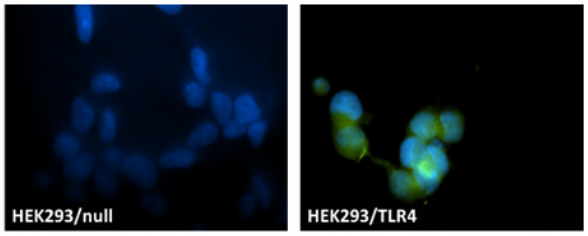
HEK293/null
HEK293/TLR4

B

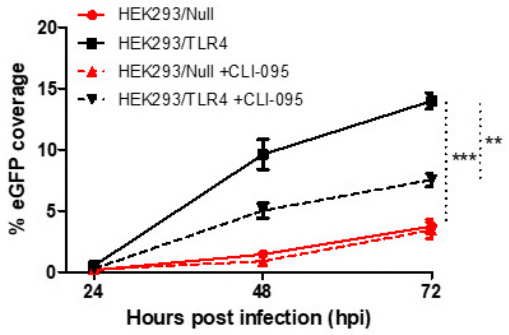
HEK293/Null
HEK293/TLR4
HEK293/Null +CLI-095
HEK293/TLR4 +CLI-095
% eGFP coverage
20
15
10
5
0
24
48
72
Hours post infection (hpi)
***
**

FIG 2

A

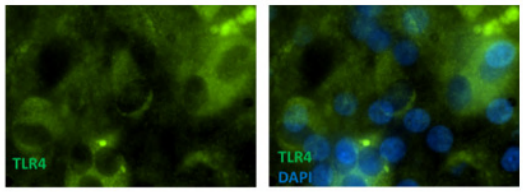
TLR4
TLR4
DAPI

B

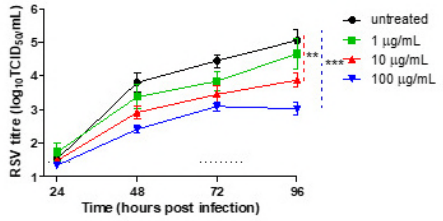
RSV titre (log10TCID50/mL)
Time (hours post infection)
untreated
1 µg/mL
10 µg/mL
100 µg/mL
**
***

C

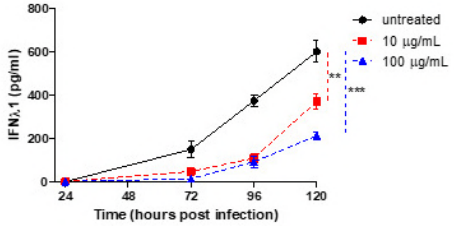
IFNλ1 (pg/ml)
Time (hours post infection)
untreated
10 µg/mL
100 µg/mL
**
***

FIG 3

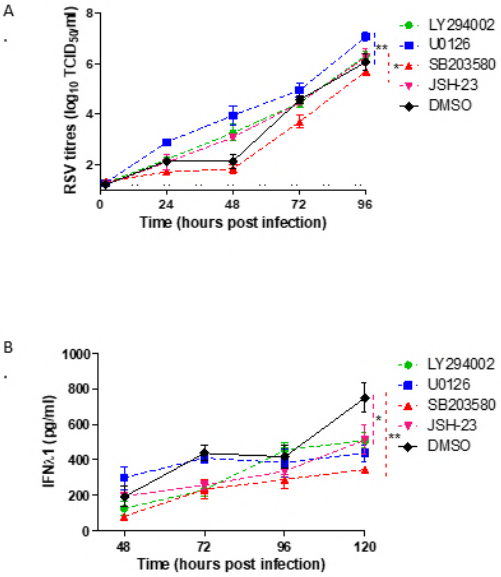
A
.
RSV titres (log10 TCID50/ml)
8
6
4
2
0
24
48
72
96
Time (hours post infection)
**
*
LY294002
U0126
SB203580
JSH-23
DMSO
B
.
IFNλ1 (pg/ml)
1000
800
600
400
200
0
48
72
96
120
Time (hours post infection)
*
**
LY294002
U0126
SB203580
JSH-23
DMSO

FIG 4

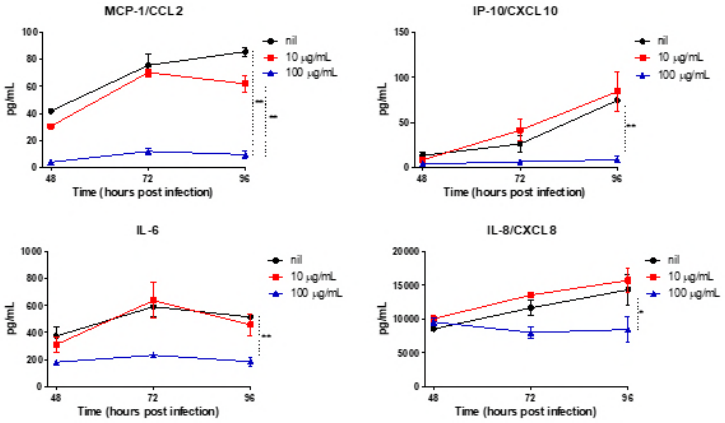
MCP-1/CCL2
IP-10/CXCL10
IL-6
IL-8/CXCL8
pg/mL
Time (hours post infection)
nil
10 μg/mL
100 μg/mL
48
72
96